A 9 megapixel large-area back-thinned CMOS sensor with high sensitivity and high frame-rate for the TAOS II program

Jérôme Pratlong[*a], Shiang-Yu Wang[b], Matthew Lehner[b], Paul Jorden[a], Paul Jerram[a], Steven Johnson[a]

[a] e2v, Waterhouse Lane, Chelmsford, Essex, CM1 2QU, UK; [b] Institute of Astronomy and Astrophysics, Academia Sinica, P.O. Box 23-141, Taipei, Taiwan.

ABSTRACT

The Transneptunian Automated Occultation Survey (TAOS II) is a robotic telescope system using three telescopes in San Pedro Martir Observatory in Mexico. It measures occultation of background stars by small TransNeptunian Objects (TNO) in order to determine their size distribution. Each telescope focal plane uses ten buttable backthinned CMOS sensors. Key performance features of the sensors are: Large array format 4608 x 1920, Pixel size 16µm, Multi ROIs, 8 analogue video channels, Frame rate of 20-40 fps [using ROIs], Low noise <3e-, Cryogenic dark current <0.1e$^-$/pixel/s, backthinned for >90% peak quantum efficiency. The paper describes top level application requirements for the TAOS II detector. The sensor design including the pixel and buttable package are described together with performance at room temperature and cryogenic temperature of backthinned devices. The key performance specifications have been demonstrated and will be presented. The production set of 40 devices are due for completion within 2017.

Keywords: TAOSII, cryogenic, CMOS, Back illumination, survey, low noise, Megapixel, focal plane.

1. INTRODUCTION

A measurement of the size distribution of small TNOs (down to D ~ 0.5km) is needed to help constrain models of the dynamical evolution of the Solar System, as well as provide important information on the origin of short-period comets. The direct detection of such objects is difficult because they are extremely faint, with typical magnitudes R > 28, and are thus invisible to surveys using even the largest telescopes. However, a small TNO will induce a detectable drop in the brightness of a distant star when it passes across the line of sight. The goal of the TAOS II[1] project is to detect such occultation events and measure the size distribution of TNOs with diameters 0.5km < D < 30km. The second goal for TAOS II project is to detect the Sedna like objects which might be related to the Oort cloud and can be few hundred to thousands of AU away from the Sun.

TAOS II will be a successor survey to the Taiwanese-American Occultation Survey (TAOS I)[2]. This survey uses four telescopes located at Lulin Observatory in central Taiwan. The system is capable of monitoring 500~1000 stars simultaneously at a cadence of 5 Hz. In order to control the false positive rate simultaneous detection of any event in three or four telescopes is required. TAOS I has been in operation since February, 2005. To date, no events have been detected. While the survey is performing better than expected in terms of sensitivity, the expected event rate turned out to be much lower than originally predicted due to a previously unmeasured break in the size distribution at D = 90km[3]. TAOS has published the strongest upper limits to date on the surface density of objects with D > 0.7km[4]. Nevertheless, while TAOS I may end up detecting several events over the coming years, it is clear that it will not be capable of providing the statistically useful number of events needed to estimate the size distribution of the faint end of the Kuiper Belt. TAOS II was thus designed with the goal of improving the expected event rate by a factor of 100.

TAOS II will operate at the Observatorio Astronomico Nacional at San Pedro Martir (SPM) in Baja California, Mexico. This site has more than 250 clear nights per year on average, which will allow improvement of the data collection rate by a factor of about 7. The TAOS II aims to solve the diffraction pattern of the occultation lightcurves at a cadence of 20 Hz or higher, which will improve the sensitivity to smaller objects. This will

increase the detected event rate by a model-dependent factor of 1 to 10. Finally, an array of 1.3 m F/4 telescopes will be used, which will significantly enhance the signal to noise ratio (SNR) performance of the survey, even after accounting for the shorter exposures used in the 20 Hz readout. The limiting magnitude (SNR= 5) on a dark night will increase from 13.5 for TAOS I to 17 for TAOS II. This should increase the number of stars that can be monitored at any time by a factor of 20 (typically 10,000 stars total). This is expected to increase the event rate by a model dependent factor of 140~1,400.

To reach the goal of sampling the photometry of 10000 stars at 20 Hz, TAOS II cameras require a new type of sensor which will allow read out sub-apertures around target stars at a cadence of 20 Hz or higher for the focal plane around 180mm in diameter.

2. AN OVERVIEW OF THE SENSOR AND ITS TECHNOLOGY

CIS113 is the e2v sensor developed for the TAOSII cameras. The architecture has been presented in detail at two CNES workshops[5,6] and the block diagram is reproduced in Figure 1. This sensor is a stitched device of 1920 columns by 4608 rows pixel area. The pixel is a 5T (Figure 2) low noise pixel of 16µm square. To speed up the frame rate the sensor has 8 parallel video channels and feature readout while acquiring the next row illustrated figure 3. The region of interest (ROI) is an important feature for this application and this device allows ROI operations per row, per column and per half pixel array (left and right). Since the array can be independently addressed left and right it allows multiple-regions of interest.
This sensor has been made with a 0.18µm Imaging CMOS process. The starting material was thick epitaxial silicon (18µm) with a high resistivity (1 kohm.cm) to give increased sensitivity at long wavelengths. The device is also back-illuminated to improve fill factor and Anti-reflection coated to minimise reflections therefore increasing further the sensor sensitivity.

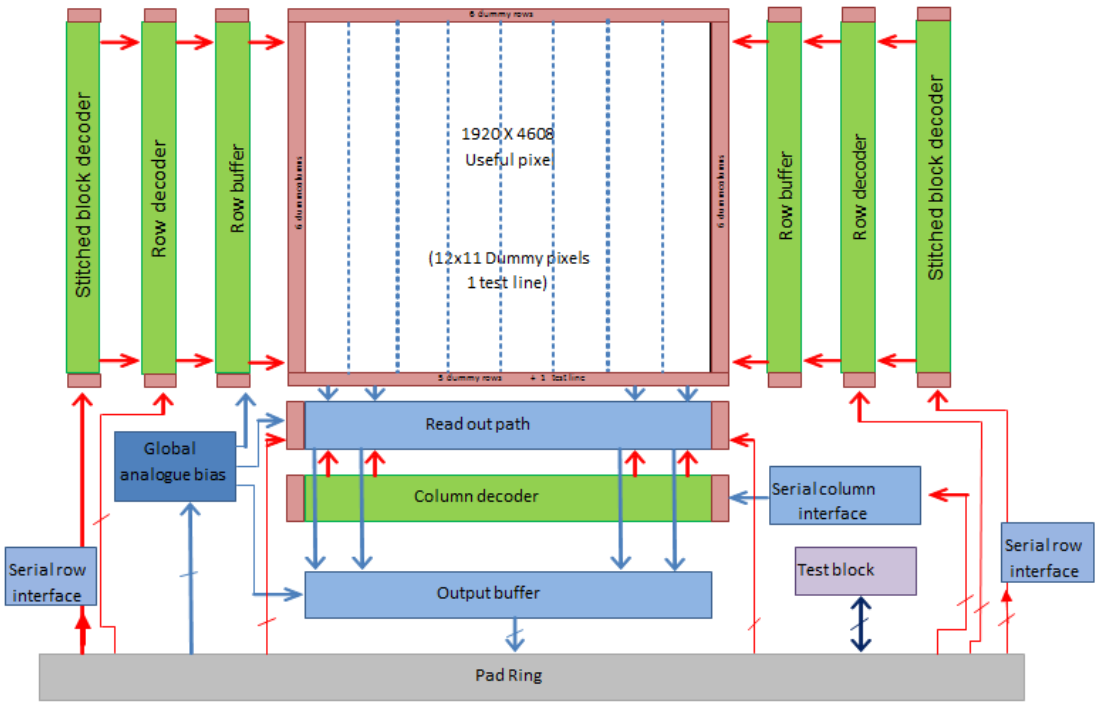

Figure 1 Sensor Architecture

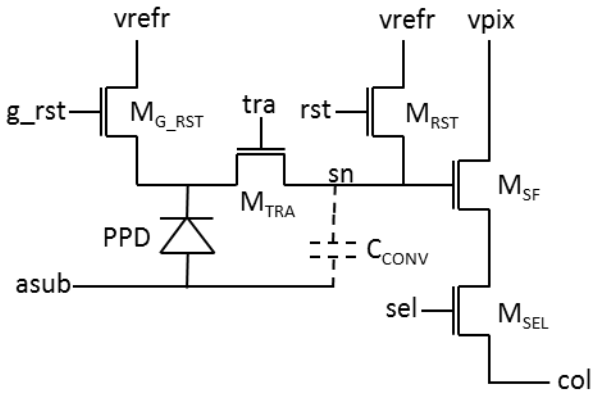

Figure 2 Pixel schematic.

Item	Description
TRANSISTORS	
M_{SF}	Nmos Source Follower amplifier transistor: low noise process.
M_{SEL}	Nmos select transistor: low noise process.
M_{TRA}	Nmos transfer transistor.
M_{RST}	Nmos reset transistor: low noise process
M_{G_RST}	Nmos global reset transistor or Nmos anti-blooming transistor.
C_{CONV}	Parasitic charge conversion capacitance
SIGNALS	
sn	Internal to the pixel sense node name
sel	Select command that connects to the gate of the transistor M_{SEL}.
tra	Transfer command that connects to the gate of the transistor M_{TRA}.
rst	Reset command that connects to the gate of the transistor M_{RST}.
g_rst	Global reset command that connects to the gate of the transistor M_{G_RST}.
col	Column connection output of the pixel. It is a common signal to all pixel from that column.
vrefr	Reset voltage level that is applied to the sense node prior to charge transfer. This supply is global to the array.
vpix	Source follower supply. This supply is global to the array.
asub	Substrate connection to minimise substrate effect due to the high resistivity material ($1kOhm.cm^{-1}$) used.

Table 1 Description of the transistor and signal used in the pixel.

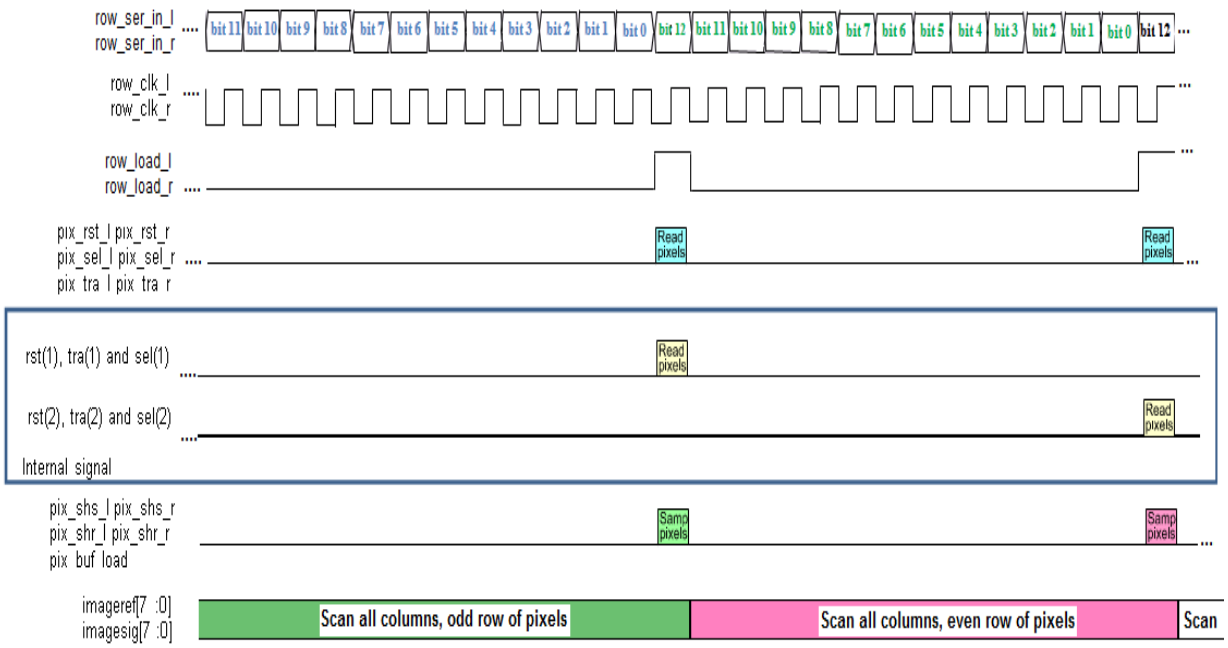

Figure 3 Example of timing access to the sensor CIS113.

3. THE FOCAL PLANE ARRANGEMENT

3.1 Focal plane organisation

CIS113 is a device that is three sides but-table for focal plane mosaic applications. The focal plane implementation for TAOSII is represented in Figure 4. The fill factor at the focal plane level is about 94%. A dedicated package with PGA (Pin Grid Array) has been designed including provision for a temperature sensor.

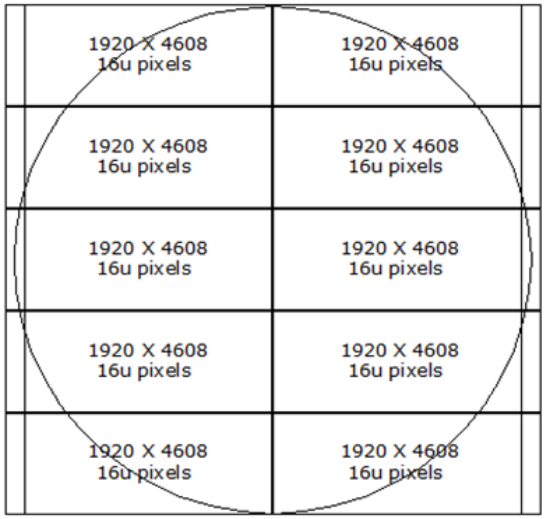

Figure 4: Focal plane arrangement.

3.2 Package

The package is designed to optimise the focal plane level fill factor and flatness. The dimensions and values are shown in figure 5 while the details of the package itself can be found in Figure 6.

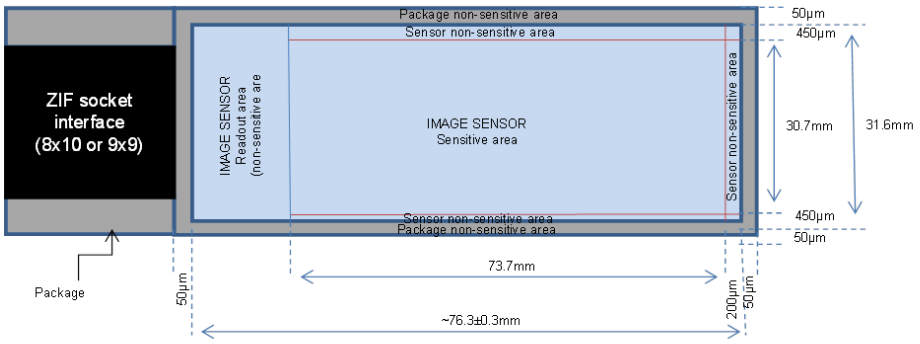

Requirement for the package:

- 3 sides buttability
- Flatness: Peak-to-Valley better than 30µm

	Value
Focal plane sensitive area only	22626mm^2
Focal plane total image area	23818mm^2
Ratio between non-sensitive area and sensitive area	
Equivalent Fill Factor at focal plane level.	94%

Figure 5: Overall dimension for highest fill factor.

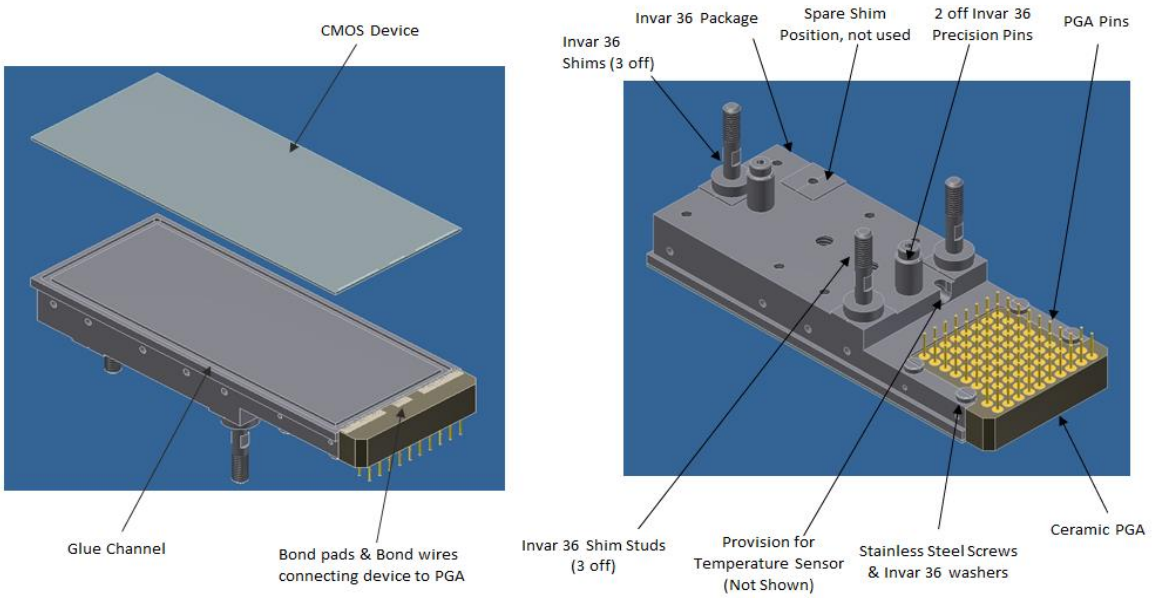

Figure 6: Details of the package.

4. TEST SETUP

4.1 Test Description

A dedicated camera was built for this program to enable low temperature characterisation. The features are shown in Figure 7. A National Instrument PXIe-5171R 8 channel oscilloscope PXI card with 250 Msps was used for the image acquisition.

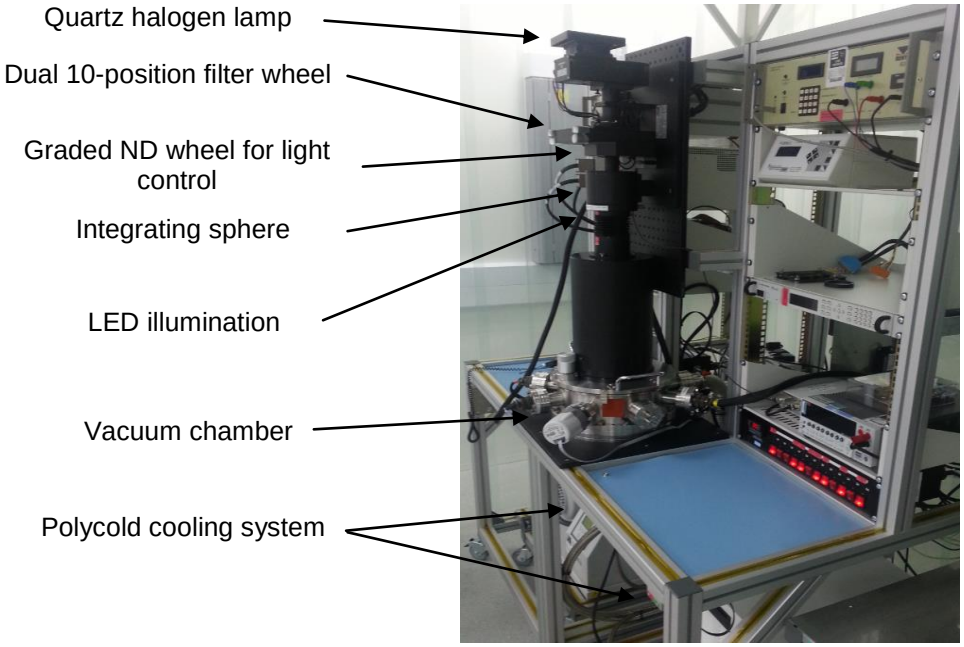

Figure 7 Camera used to characterise CIS113 for TAOSII program.

Figure 8 illustrates a sample and the sensor attached to its handling jig.

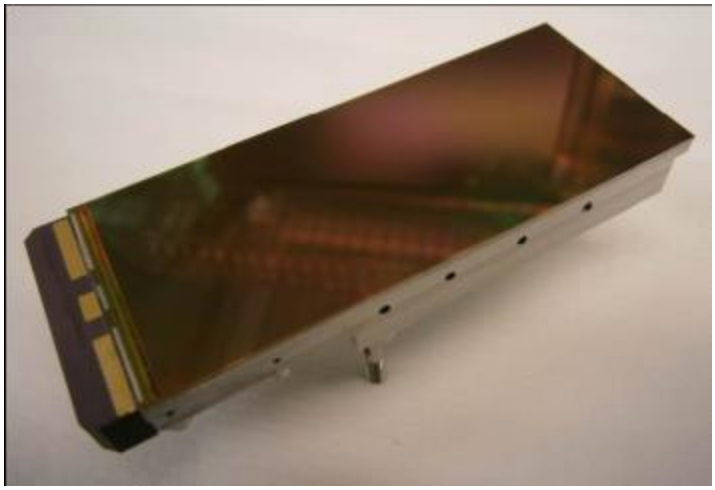

(a)

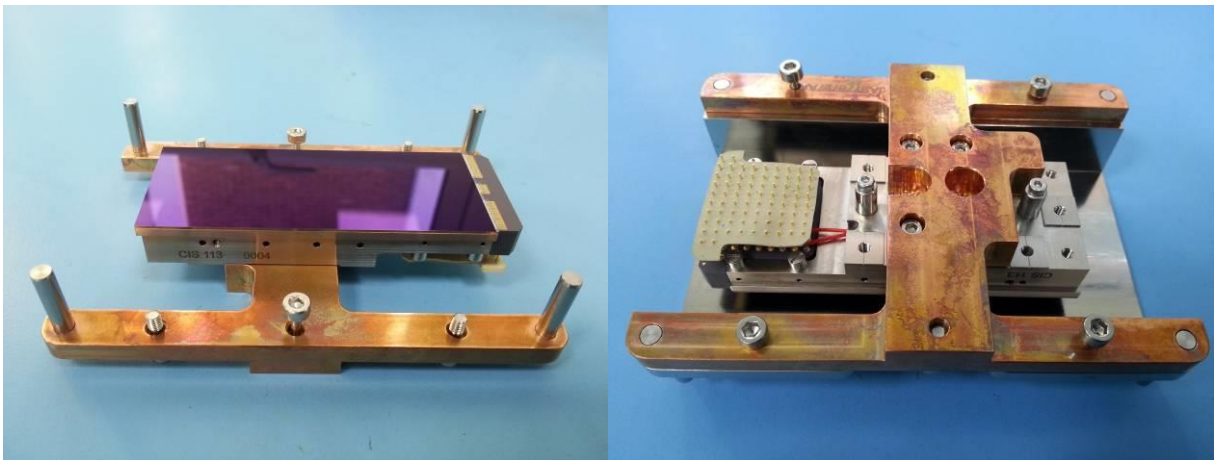

(b)

Figure 8 (a) back-illuminated CIS113 sample (b) underside of device in handling jig.

4.2 Thermal control

The EO (Electro-Optical) tests were repeated on the device under vacuum cooling the device down to -132 °C. The temperature of the cold finger was set and the temperature of the device was measured by the thermistor fitted within the package. The comparison chart of the set cold finger temperature to the device temperature is shown in Figure 9.

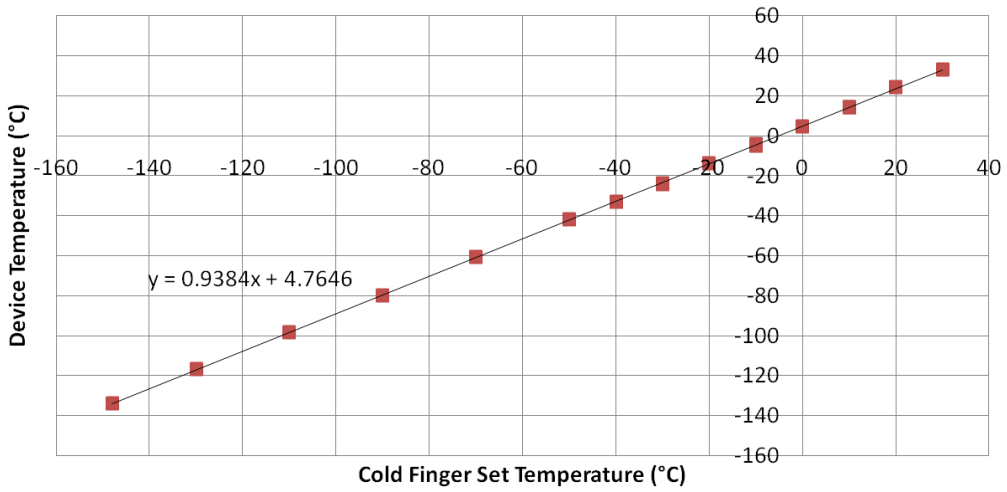

Figure 9 Temperature calibration.

5. TEST RESULTS

5.1 Irradiance response

The sensor noise floor is critical to the application therefore it was important to cool down the device in order to minimise the impact of the dark current. First the photo-response (Figure 10) curve has been measured versus temperature in order to extract key characteristics of the sensor such as linearity, CVF (conversion voltage Factor) and linear capacity. The sensor has been found to perform down to temperature below -130°C.

Linear capacity (charge integrated at the sense node within linearity criteria) is stable over a large temperature range (Figure 11) this can be explained by the fact that this parameter is limited by the sense node and not the photodiode. At sense node level the reset applied is not a function of temperature. This is also confirmed by the non-linearity (1st order fitting) in Figure 10.
The CVF (conversion voltage factor) increases with temperature (see Figure 11). Below -100^{o}C the CVF seems to flatten. The slope between 0 and -100^{o}C gives a CVF variation of about -0.10% per degree Celsius. This is similar to e2v CCD results.

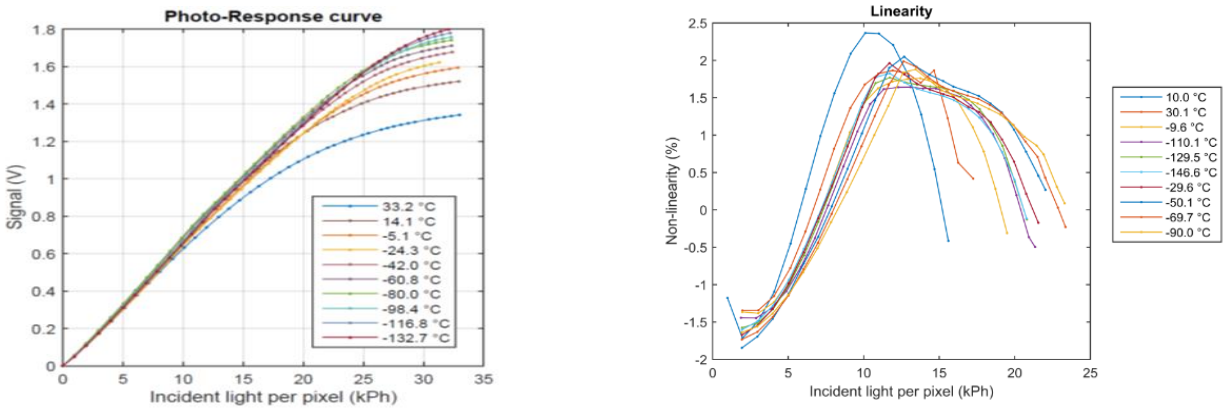

Figure 10 Photo-response and linearity versus temperqature.

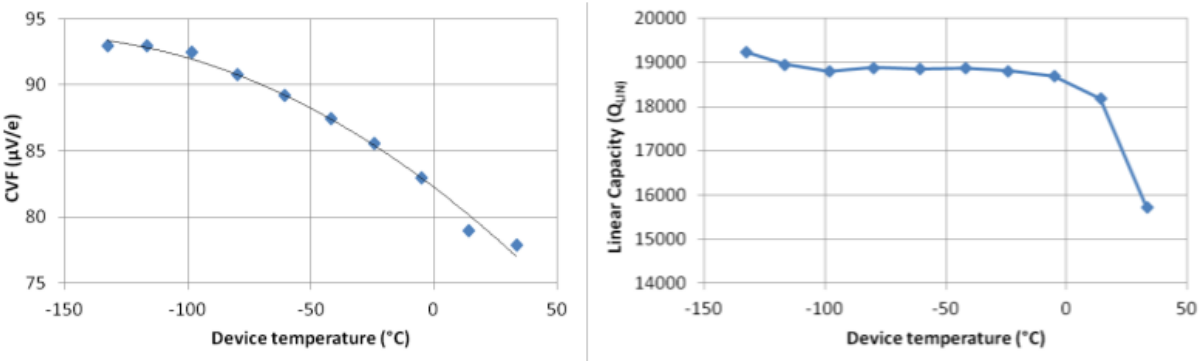

Figure 11 CVF and Q_{LIN} versus temperature.

5.2 Dark current

The dark current measurement versus temperature is reported in Figure 12. These values are acquired in rolling shutter mode hence there is no sense node dark current contribution. The activation energy is extracted from the Arrhenius plot (Figure 12) and is 1.12eV. This is the same value than the band-gap energy of the silicon. This implies that the dark current is dominated in the pinned photodiode (PPD) by the diffusion current and that there is no defect. Defects can present in the case of hot pixels or can occur for space missions due to proton radiation. In this case the activation energy will vary. This result also implies that there is no contribution from the surface of the PPD as this would be from mid-band traps. This is expected since the photodiode is pinned. There is also no contribution from any Gate-Induced-leakage (GIL).
As mentioned earlier in this paper this device is back illuminated. The energy activation of 1.12eV also indicates that there is no contribution from the back surface to the dark current.

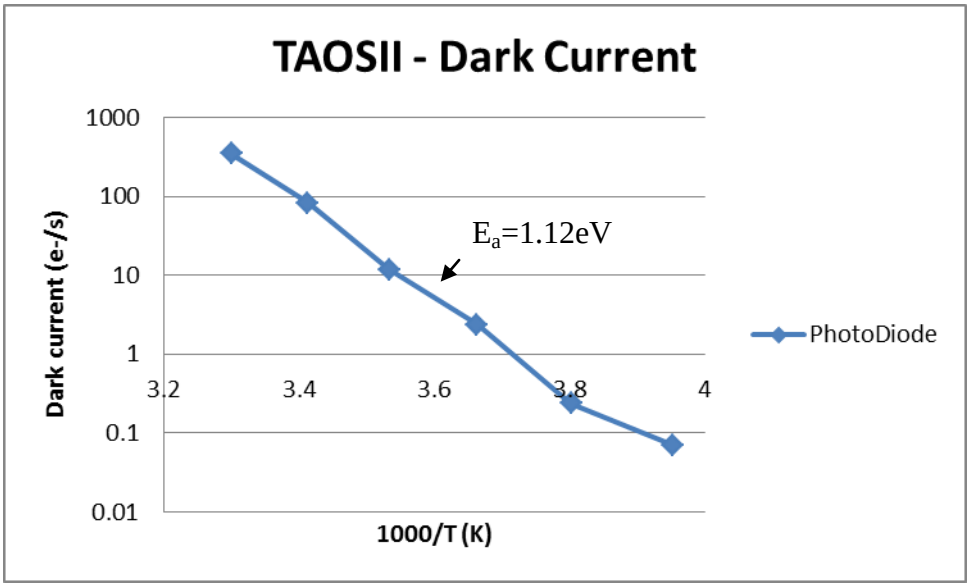

Figure 12 Dark current Arrhenius plot.

5.3 Readout noise

The readout noise in µV without dark current has been measured and it is reported in Figure 14. The results show the noise floor (in µV) increases with decreasing temperature. For this sensor the noise is dominated by the in-pixel source follower 1/f noise, the rest being due to the CDS sample-and-hold kTC noise and the white noise of the readout path.
The pixel output noise (V_n) derives from the integration of the drain current noise (I_n) with the output impedance $1/g_m$, taking into account the gain due to the in-pixel source follower drain gate-source capacitance C_{GS} to all other parasitic components comprising the sense node capacitance C_{SN}[7], as shown in Figure 13. For a given size of transistor and hence given C_{GS}, as the sense node capacitance C_{SN} decreases, the gain applied to the 1/f noise of the in-pixel source follower increases.

Note from Figure 11 that the CVF increases as the temperature is reduced which implies that the sense node capacitance decreases. The noise floor from the in-pixel source follower is known to be a function of this capacitance due to the C_{GS} feedback capacitance. The CVF has increased by 10% from 35 to -25 ^{o}C. In the same temperature range the noise has increased by 14%. Then a large increase of the noise in µV is down to the decrease of the sense node capacitance. In order to take into account the variation of sensitivity, in Figure 15 the read-out noise is plotted in electrons. The read noise in electrons is constant from 35^{o}C down to -25^{o}C which again confirms the relationship between sensitivity and noise in µV. Since the signal charge

handled within the non-linearity criteria, as shown in Figure 10, also remains a constant with temperature, then the dynamic range is also constant with temperature.

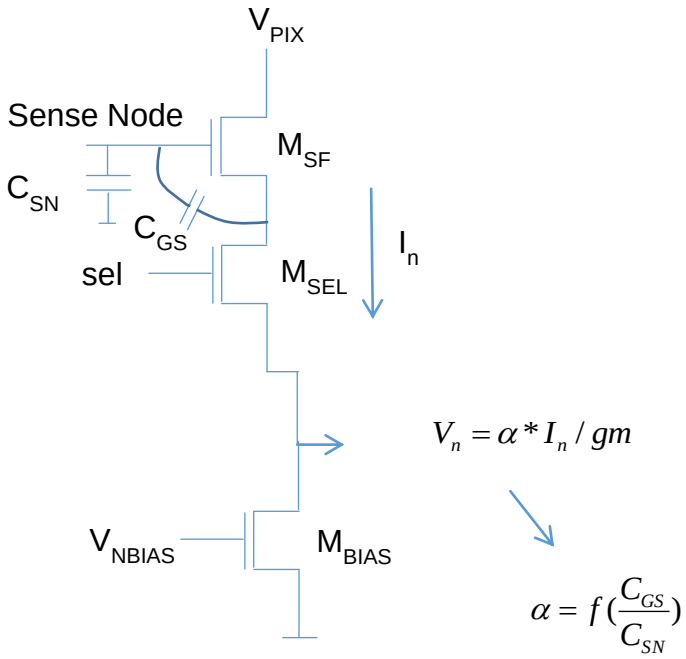

Figure 13 In-pixel amplifier and feedback.

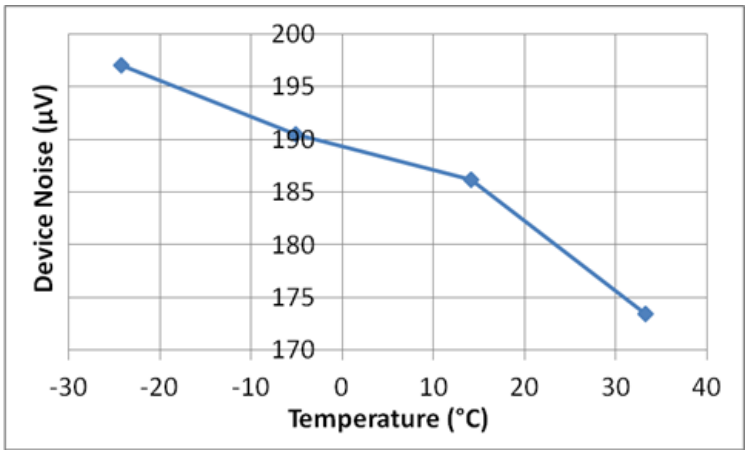

Figure 14 Readout noise in μV_{RMS} versus temperature.

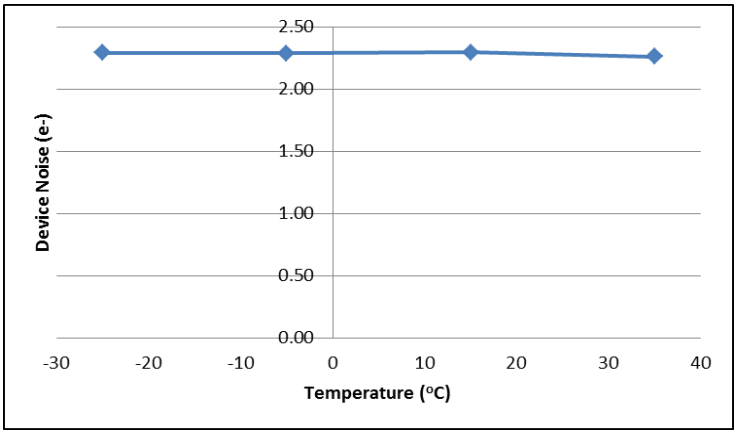

Figure 15 Read-out noise in electrons versus temperature.

5.4 Blooming

The blooming test is generally performed by illuminating a small area of the device with increasing light levels using a spatial mask, in this case 50x50. The device normally saturates at 30 kPh (kilo-photons) and the illuminated level reached 98 kPh. From the results shown in Figure 16, it is clear that, charge does not spread from the pixels (i.e. bloom) when the device is oversaturated. This is because the 5th transistor acts as an anti-blooming drain.

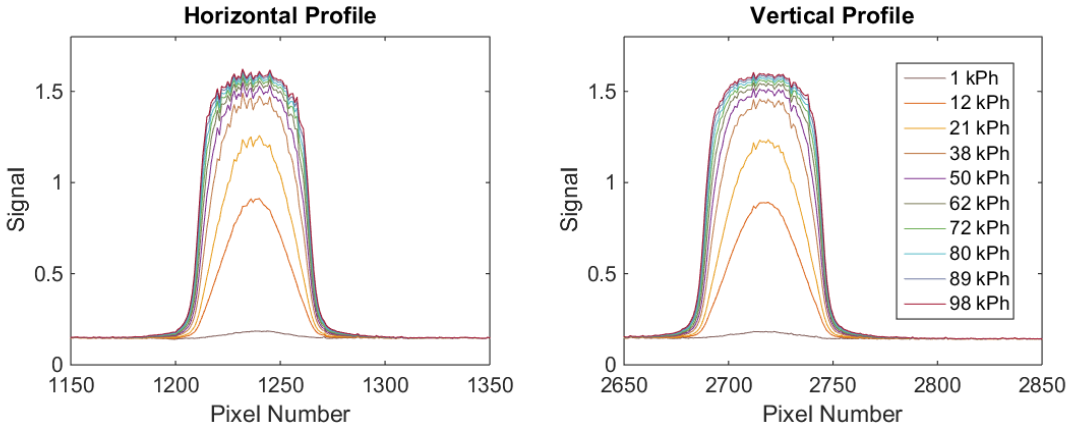

Figure 16 Blooming results in both directions.

6. SUMMARY

The behaviour of the sensor CIS113 to be used within the program TAOSII has been presented. Particular attention has been given to the temperature effects with the following conclusions:

- CIS113 back-illuminated sensors were found to function down below -130^{o}C.
- The CVF behaviour is similar to a typical e2v CCD: namely -0.10% change per degree Celsius.
- The noise floor of 2.4 e^{-} was constant over temperature.
- The dark current variation with temperature behaves as expected, with a shot noise becoming equivalent to the read noise at 0^{o}C and negligible for the TAOS application below -5^{o}C.
- The dynamic range is constant over temperature as a result of both the noise floor and the linear signal charge handling being constant over temperature.

7. ACKNOWLEDGEMENT

We gratefully acknowledge support from the Academia Sinica of Taiwan for the TAOS II project.

8. REFERENCES

[1] Lehner, M. J. et al., "The Transneptunian Automated Occultation Survey (TAOS II)," Proc. SPIE 8444, 84440D-2 (2012).
[2] Lehner, M. J.et al., "The Taiwanese-American Occultation Survey: The Multi-Telescope Robotic Observatory," PASP 121, 138–152 (2009).
[3] Bernstein, G. M. et al., "The Size Distribution of Trans-Neptunian Bodies," AJ 128, 1364–1390 (2004).
[4] Zhang, Z.-W. et al., "The TAOS Project: Results from Seven Years of Survey Data," AJ 146, 14, (2013).
[5] Pratlong J. et al., "TAOS II: Three 88-Megapixel astronomy arrays of large area, backthinned, and low-noise CMOS sensors," CNES workshop (2013).
[6] Johnson S. et al. "Low temperature measurements of the large-area, backthinned, and low-noise TAOSII CMOS sensors," CNES workshop (2015).
[7] BoukhaymaA. Et al. "Comparison of two optimized readout chains for low light CIS," proc of SPIE 9022, 9022OH-1(2014).